

Double-diffusive interleaving due to horizontal gradients

By JUDITH Y. HOLYER

School of Mathematics, University of Bristol, England

(Received 21 February 1983 and in revised form 31 August 1983)

In this paper we present a linear stability analysis for an unbounded, vertically stratified fluid which has compensating horizontal temperature and salinity gradients, so there is no horizontal density gradient. We obtain the most unstable perturbation for given linear horizontal and vertical gradients and calculate the growth rates, the vertical lengthscale of the intrusion and the slope of the intrusion to the horizontal. We show that the system is most unstable to two-dimensional disturbances and that, except for a small region in which the temperature stratification is unstable and the salinity stratification is stable, the most-unstable disturbance is non-oscillatory. We also obtain a solution to the fully nonlinear equations and calculate the fluxes of heat and salt. The nonlinear solution shows that alternating interfaces of salt-finger and diffusive interfaces will eventually appear on the intrusion when the vertical stratifications are both stable.

1. Introduction

It is now recognized that there are several mechanisms that can lead to the formation of layers in the temperature and salinity fields in the ocean. In this paper we investigate how layers may be set up owing to the presence of horizontal gradients, in order to gain a better understanding of the interleaving that can occur at oceanic fronts. Layers that probably owe their existence to the presence of horizontal gradients have been seen in the observations of Stommel & Fedorov (1967), Horne (1978) and Gregg (1975, 1979) amongst others. It is observed that in these regions the temperature and salinity gradients are compensating and the density surfaces are almost horizontal.

Laboratory experiments of Thorpe, Hutt & Soulsby (1969), Wirtz, Briggs & Chen (1972) and Ruddick & Turner (1979) demonstrate that stratified fluids with horizontal gradients of temperature and salinity are unstable to horizontal interleaving. Previous theoretical work (Stern 1967; Toole & Georgi 1981) assumes that it is necessary to have salt fingers in order to obtain the interleaving instability. Toole & Georgi assume that the fluxes of heat and salt in the vertical are dominated by transports due to the presence of salt fingers. They model the fluxes by using uniform eddy diffusivities and by taking the ratio of the fluxes of heat and salt to be equal to a constant, γ . In this paper we start from the state of rest and show that purely molecular processes will lead to the growth of the interleaving instability. The instability is shown to grow until the vertical gradients of temperature and salinity caused by the interleaving are large enough to set up diffusive and salt-finger interfaces on the intrusions. This paper presents a study of the process by which the interleaving appears. The earlier work has examined, in a heuristic manner, the later stages of development of the instability when the interleaving has itself become

unstable and has acquired salt-finger and diffusive interfaces. The results of Toole & Georgi can be obtained from this paper, for the non-rotating case, by replacing the molecular diffusivities used here with the eddy diffusivities that they use.

The model presented here allows for linear horizontal and vertical gradients of temperature and salinity. We consider flow in an unbounded fluid, since for oceanic problems the boundaries are usually a long way away, compared with the scale of the intrusion. The scales are then determined by the fluid properties, just as they are for salt fingers in an unbounded fluid (Walin 1964). In §2 we present the linear stability analysis for an unbounded region of incompressible fluid and obtain the characteristic equation for the growth of periodic perturbations. In §3 we find the solutions of this equation which have maximum growth rates for given temperature and salinity gradients. We obtain the lengthscale of intrusions and their slope to the horizontal corresponding to the maximum growth rates. In §4 we find the flux ratio corresponding to the maximum growth rate. In §5 we obtain a solution to the fully nonlinear equations. This solution shows that if both vertical stratifications are initially stable then the instability will grow and when it is large enough salt-finger and diffusive interfaces will appear on the intrusion. These interfaces are maintained by the instability and they can be seen in the experiments of Ruddick & Turner (1979).

2. Linear stability analysis

Suppose we have an unbounded region of incompressible fluid, which contains both temperature and salinity variations. We suppose that there is no horizontal variation in the density field, so that the temperature and salinity fields compensate each other horizontally. The vertical temperature and salinity gradients may be stable or unstable. The situation that is particularly interesting is when both the temperature and salinity gradients are vertically stable, so that the temperature increases with height and the salinity decreases with height. Even in this apparently stable situation the horizontal temperature and salinity gradients drive an instability. This instability leads to the interleaving that is seen in the laboratory experiments of Ruddick & Turner (1979) and it is likely that it is sometimes responsible for finestructure layering in the ocean (see Fedorov 1978).

The coordinates are chosen with z measuring distance vertically upwards and x horizontal. We show in the appendix that there is a Squires transformation for this system and use it to show that the system has the largest growth rates for two-dimensional perturbations. We therefore consider only two-dimensional perturbations. We suppose that the temperature and salinity fields have linear horizontal and vertical gradients, so that the undisturbed temperature and salinity fields are given by

$$T_0 + \bar{T}_x x + \bar{T}_z z, \quad S_0 + \bar{S}_x x + \bar{S}_z z. \quad (2.1)$$

We suppose that the density field is given by

$$\rho = \rho_0(1 - \alpha T + \beta S), \quad (2.2)$$

where T and S are the temperature and salinity, and α and β are the coefficients of expansion for heat and salt, defined so that α and β are both positive. We require that there is no horizontal variation of the undisturbed density field, so

$$\alpha \bar{T}_x = \beta \bar{S}_x. \quad (2.3)$$

We shall always assume $\bar{S}_x > 0$, i.e. the x -direction is in the direction of increasing salinity. The stream function ψ is defined by

$$u = -\frac{\partial\psi}{\partial z}, \quad w = \frac{\partial\psi}{\partial x}, \quad (2.4)$$

where u is the horizontal velocity and w is the vertical velocity. The perturbations to the temperature, salinity and pressure fields are T , S and p . The linearized equations for vorticity, temperature, salinity and pressure are then

$$\frac{\partial}{\partial t} \nabla^2 \psi = \frac{\partial}{\partial x} (g(\alpha T - \beta S)) + \nu \nabla^4 \psi, \quad (2.5a)$$

$$\frac{\partial T}{\partial t} + \frac{\partial\psi}{\partial x} \bar{T}_z - \frac{\partial\psi}{\partial z} \bar{T}_x = \kappa_T \nabla^2 T, \quad (2.5b)$$

$$\frac{\partial S}{\partial t} + \frac{\partial\psi}{\partial x} \bar{S}_z - \frac{\partial\psi}{\partial z} \bar{S}_x = \kappa_S \nabla^2 S, \quad (2.5c)$$

$$\nabla^2 p = \rho_0 g \frac{\partial}{\partial z} (\alpha T - \beta S). \quad (2.5d)$$

These equations are easily manipulated to obtain an equation for ψ :

$$\begin{aligned} & \left(\frac{\partial}{\partial t} - \kappa_T \nabla^2 \right) \left(\frac{\partial}{\partial t} - h\nu \nabla^2 \right) \left(\frac{\partial}{\partial t} - \kappa_S \nabla^2 \right) \nabla^2 \psi \\ &= -g\alpha \bar{T}_z \left(\frac{\partial}{\partial t} - \kappa_S \nabla^2 \right) \frac{\partial^2 \psi}{\partial x^2} + g\beta \bar{S}_z \left(\frac{\partial}{\partial t} - \kappa_T \nabla^2 \right) \frac{\partial^2 \psi}{\partial x^2} + g\beta \bar{S}_x (\kappa_T - \kappa_S) \nabla^2 \frac{\partial^2 \psi}{\partial x \partial z}. \end{aligned} \quad (2.6)$$

This is a linear equation with constant coefficients and so the solution will be a superposition of solutions of the form

$$\psi = \text{Re} \{ \psi_0 \exp(i(kx + mz) + \lambda t) \}, \quad (2.7)$$

where ψ_0 is a complex constant, k and m are the horizontal and vertical wavenumbers, the real part of λ is the growth rate and the imaginary part of λ is the frequency. Substituting this solution into (2.6) yields the characteristic equation

$$\begin{aligned} & (\lambda + \nu\mu^2) (\lambda + \kappa_T \mu^2) (\lambda + \kappa_S \mu^2) \mu^2 + \lambda g k^2 (\alpha \bar{T}_z - \beta \bar{S}_z) \\ &+ g k^2 \mu^2 \kappa_S \kappa_T \left(\frac{\alpha \bar{T}_z}{\kappa_T} - \frac{\beta \bar{S}_z}{\kappa_S} \right) + g \beta \bar{S}_x (\kappa_T - \kappa_S) k m \mu^2 = 0, \end{aligned} \quad (2.8)$$

where $\mu = (k^2 + m^2)^{1/2}$ is the absolute wavenumber. The solution (2.7) is then unstable if $\text{Re}(\lambda) > 0$. Neutral stability occurs if $\lambda = 0$ or if λ is pure imaginary (so $\lambda = i\omega$).

(i) If $\lambda = 0$, substituting into (2.8) gives

$$\nu \kappa_S \kappa_T \mu^6 = -g k^2 \kappa_S \kappa_T \left(\frac{\alpha \bar{T}_z}{\kappa_T} - \frac{\beta \bar{S}_z}{\kappa_S} \right) - g \beta \bar{S}_x (\kappa_T - \kappa_S) k m. \quad (2.9)$$

If $\bar{S}_x \neq 0$ there is always a solution to this when

$$\beta \bar{S}_x (\kappa_T - \kappa_S) \frac{m}{k} < \kappa_S \kappa_T \left(\frac{\beta \bar{S}_z}{\kappa_S} - \frac{\alpha \bar{T}_z}{\kappa_T} \right). \quad (2.10)$$

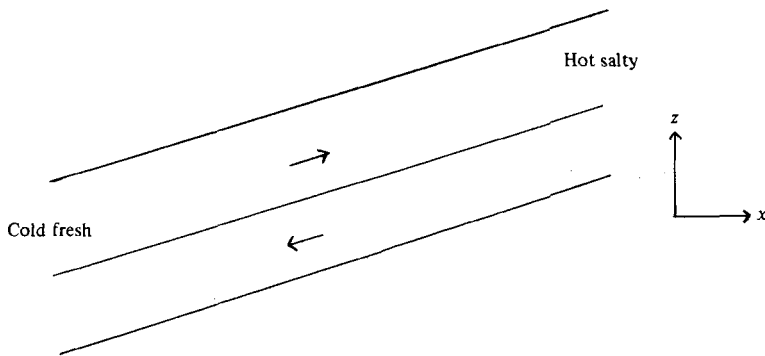


FIGURE 1. Schematic illustration of slope of wavefronts for the direct mode of instability, when the vertical gradients are stable.

There are always values of m/k for which this condition holds and hence, by choosing μ smaller than the value given by (2.9), the system will always be unstable. If $\alpha\bar{T}_z > 0$ and $\beta\bar{S}_z < 0$, so that both components are vertically stable, then (2.10) gives $m/k < 0$ (since $\bar{S}_x > 0$ and $\kappa_T > \kappa_S$). This means that the wavefronts tilt as shown in figure 1, with the result that hot salty fluid lies above cold fresh fluid between any wavefronts. This situation is analogous to the salt-finger regime when there are vertical gradients. There is experimental evidence that wavefronts do slope in this direction (Thorpe *et al.* 1969). If $\bar{S}_x = 0$ there is only a solution to (2.9) when $\beta\bar{S}_z/\kappa_S > \alpha\bar{T}_z/\kappa_T$. If $\alpha\bar{T}_z < \beta\bar{S}_z$, so that the system would be unstable in the absence of any dissipation, then, since $\kappa_S < \kappa_T$, there is always a direct instability. If $\alpha\bar{T}_z > \beta\bar{S}_z$ then there is only an instability if $\beta\bar{S}_z/\kappa_S > \alpha\bar{T}_z/\kappa_T$. This is the condition for the existence of salt-fingering in an unbounded region (Walén 1964). As \bar{S}_x increases from zero, the interleaving instability immediately starts to grow.

(ii) If $\lambda = i\omega$, with ω real, there is a transition to an oscillatory instability. Substituting into (2.8) and equating real and imaginary parts gives

$$\begin{aligned} \omega^2 &= \frac{gk^2}{\mu^2} (\alpha\bar{T}_z - \beta\bar{S}_z) + (\nu\kappa_T + \nu\kappa_S + \kappa_S\kappa_T) \mu^4 \\ &= \frac{1}{\nu + \kappa_T + \kappa_S} \left[\nu\kappa_T\kappa_S\mu^4 + g\beta\bar{S}_x(\kappa_T - \kappa_S) \frac{km}{\mu^2} + \frac{gk^2}{\mu^2} \kappa_S\kappa_T \left(\frac{\alpha\bar{T}_z}{\kappa_T} - \frac{\beta\bar{S}_z}{\kappa_S} \right) \right]. \end{aligned} \quad (2.11)$$

In order for (2.11) to have a solution, it is necessary that $\mu^2 > 0$, with ω real. This requirement gives two conditions. First $\mu^2 > 0$ requires that

$$\beta\bar{S}_x(\kappa_T - \kappa_S) \frac{m}{k} > \alpha\bar{T}_z(\nu + \kappa_T) - \beta\bar{S}_z(\nu + \kappa_S), \quad (2.12)$$

and secondly $\omega^2 > 0$ requires that

$$\beta\bar{S}_x(\kappa_T - \kappa_S) (\nu\kappa_T + \nu\kappa_S + \kappa_S\kappa_T) \frac{m}{k} > (\nu + \kappa_S) \kappa_T^2 \beta\bar{S}_z - (\nu + \kappa_T) \kappa_S^2 \alpha\bar{T}_z. \quad (2.13)$$

If $\alpha\bar{T}_z - \beta\bar{S}_z > 0$, so that the vertical stratification is statically stable, then condition (2.12) implies that condition (2.13) is also true. If $\alpha\bar{T}_z - \beta\bar{S}_z < 0$ then condition (2.13) implies condition (2.12). The values of m/k can always be chosen so that there is an oscillatory instability. In the case where $\alpha\bar{T}_z > 0$ and $\beta\bar{S}_z < 0$, then (2.12) gives $m/k > 0$, so the wavefronts tilt in the opposite direction to their tilt in the stationary

instability. If $\bar{S}_x = 0$, then, using (2.12) and (2.13), there can only be oscillatory instability when $\alpha\bar{T}_z < 0$ and $\beta\bar{S}_z < 0$, so the temperature gradient is unstable and the salinity gradient stable. In this case the oscillatory instability can only occur when

$$\frac{\nu + \kappa_S}{\nu + \kappa_T} < \frac{\alpha\bar{T}_z}{\beta\bar{S}_z} < \frac{(\nu + \kappa_S)\kappa_T^2}{(\nu + \kappa_T)\kappa_S^2}. \quad (2.14)$$

For short waves, i.e. $\mu \rightarrow \infty$, the values of λ obtained from (2.8) are $-\nu\mu^2$, $-\kappa_T\mu^2$ and $-\kappa_S\mu^2$. Hence short waves always decay. For long waves, i.e. $\mu \rightarrow 0$, the diffusion ceases to be important and (2.8) has the solution

$$\lambda^2 = -\frac{gk^2}{\mu^2}(\alpha\bar{T}_z - \beta\bar{S}_z). \quad (2.15)$$

If $\alpha\bar{T}_z > \beta\bar{S}_z$ then λ is pure imaginary and equal to the buoyancy frequency of the fluid, so long waves propagate through the fluid like internal waves in a non-dissipative fluid. If $\alpha\bar{T}_z < \beta\bar{S}_z$ then the fluid is top-heavy and (2.15) gives the initial growth rate for the overturning of the fluid. This growth will be maximum if $m = 0$, so the fluid moves directly downwards. This is the standard convective instability, which always occurs on the largest available lengthscale. This instability only depends on the fluid being top-heavy. It exists in the absence of diffusion. The double-diffusive instability, that leads to interleaving, occurs for $\alpha\bar{T}_z > \beta\bar{S}_z$, i.e. when the fluid is bottom-heavy.

3. The most-unstable mode for given gradients

We have seen in §2 that in the presence of horizontal temperature and salinity gradients the fluid is unstable for any vertical distribution of temperature and salinity. In this section we find the maximum growth rates of this instability and the wavenumbers and wavefront slopes associated with the maximum growth rates.

If the growth rate $\text{Re}(\lambda)$ is maximum then, if λ is real so the instability is non-oscillatory, the maximum growth occurs when

$$\frac{\partial \lambda}{\partial k} = \frac{\partial \lambda}{\partial m} = 0. \quad (3.1)$$

Hence for non-oscillatory modes the maximum growth is obtained by differentiating the characteristic equation (2.8). This leads to two equations, which should be solved with (2.8) to find the values of λ , k and m for maximum growth:

$$\lambda^2(\nu + \kappa_T + \kappa_S) + 2\lambda\mu^2(\nu\kappa_T + \nu\kappa_S + \kappa_S\kappa_T) + 3\nu\kappa_T\kappa_S\mu^4 - \lambda g \frac{k^2}{\mu^4}(\alpha\bar{T}_z - \beta\bar{S}_z) + \frac{g\beta\bar{S}_x(\kappa_T - \kappa_S)k}{2m} = 0, \quad (3.2)$$

$$\lambda \frac{g(\alpha\bar{T}_z - \beta\bar{S}_z)}{\mu^2} = -g\kappa_S\kappa_T \left(\frac{\alpha\bar{T}_z}{\kappa_T} - \frac{\beta\bar{S}_z}{\kappa_S} \right) - \frac{g\beta\bar{S}_x}{2km}(\kappa_T - \kappa_S)(m^2 - k^2). \quad (3.3)$$

For the oscillatory modes when $\lambda = \lambda_r + i\omega$ with ω non-zero, the maximum growth occurs when

$$\frac{\partial \lambda_r}{\partial k} = \frac{\partial \lambda_r}{\partial m} = 0. \quad (3.4)$$

Taking real and imaginary parts in (2.8) leads to two equations (if $\omega \neq 0$):

$$\omega^2 = 3\lambda_r^2 + 2\lambda_r \mu^2 (\nu + \kappa_T + \kappa_S) + \mu^4 (\nu \kappa_T + \nu \kappa_S + \kappa_S \kappa_T) + \frac{gk^2}{\mu^2} (\alpha \bar{T}_z - \beta \bar{S}_z), \quad (3.5)$$

$$\begin{aligned} & 8\lambda_r^3 + 8\lambda_r^2 \mu^2 (\nu + \kappa_T + \kappa_S) + 2\lambda_r \mu^4 [(\nu + \kappa_T + \kappa_S)^2 + (\nu \kappa_T + \nu \kappa_S + \kappa_S \kappa_T)] \\ & + \mu^6 [(\nu + \kappa_T + \kappa_S) (\nu \kappa_T + \nu \kappa_S + \kappa_S \kappa_T) - \nu \kappa_S \kappa_T] \\ & + 2\lambda_r \frac{gk^2}{\mu^2} (\alpha \bar{T}_z - \beta \bar{S}_z) + gk^2 \alpha \bar{T}_z (\nu + \kappa_T) - gk^2 \beta \bar{S}_z (\nu + \kappa_S) - g\beta \bar{S}_z (\kappa_T - \kappa_S) km = 0. \end{aligned} \quad (3.6)$$

Differentiating (3.6) with respect to k and m , to find the maximum growths, gives

$$\begin{aligned} & 8\lambda_r^2 (\nu + \kappa_T + \kappa_S) + 4\lambda_r \mu^2 [(\nu + \kappa_T + \kappa_S)^2 + (\nu \kappa_T + \nu \kappa_S + \kappa_S \kappa_T)] \\ & + 3\mu^4 [(\nu + \kappa_T + \kappa_S) (\nu \kappa_T + \nu \kappa_S + \kappa_S \kappa_T) - \nu \kappa_S \kappa_T] \\ & - 2\lambda_r g (\alpha \bar{T}_z - \beta \bar{S}_z) \frac{k^2}{\mu^4} - \frac{g\beta \bar{S}_z (\kappa_T - \kappa_S) k}{2m} = 0, \end{aligned} \quad (3.7)$$

$$\frac{2\lambda_r g (\alpha \bar{T}_z - \beta \bar{S}_z)}{\mu^2} = g\beta \bar{S}_z (\nu + \kappa_S) - g\alpha \bar{T}_z (\nu + \kappa_T) + \frac{g\beta \bar{S}_z (\kappa_T - \kappa_S) (m^2 - k^2)}{2km}. \quad (3.8)$$

We now non-dimensionalize the equations for maximum growth. We define

$$q = \frac{\lambda}{\kappa_T \mu^2}, \quad H = \frac{g\beta \bar{S}_z}{\nu \kappa_T \mu^4}, \quad R_T = \frac{g\alpha \bar{T}_z}{\nu \kappa_T \mu^4}, \quad R_S = \frac{g\beta \bar{S}_z}{\nu \kappa_T \mu^4}, \quad (3.9)$$

where H is a horizontal Rayleigh number, R_T is a thermal Rayleigh number and R_S is a saline Rayleigh number. We also define

$$\sigma = \frac{\nu}{\kappa_T}, \quad \tau = \frac{\kappa_S}{\kappa_T}, \quad (3.10)$$

where σ is the Prandtl number and τ the ratio of the saline diffusivity to the thermal diffusivity.

Then for the non-oscillatory modes we obtain, by rearranging (2.8), (3.2) and (3.3), the following three equations for maximum growth:

$$H = -2 \frac{m}{k} \frac{1}{\sigma(1-\tau)} (q + \sigma) (q + 1) (q + \tau), \quad (3.11a)$$

$$R_T = \frac{\mu^2}{k^2} \frac{q + 1}{\sigma q (1 - \tau)} \left[-q^3 + q(\sigma\tau + \sigma + \tau) + 2\sigma\tau + \frac{k^2 - m^2}{\mu^2} q(q + \sigma) (q + \tau) \right], \quad (3.11b)$$

$$R_S = \frac{\mu^2 (q + \tau)}{k^2 \sigma q (1 - \tau)} \left[-q^3 + q(\sigma\tau + \sigma + \tau) + 2\sigma\tau + \frac{k^2 - m^2}{\mu^2} q(q + \sigma) (q + 1) \right]. \quad (3.11c)$$

For the oscillatory mode with maximum growth we obtain

$$H = 2 \frac{m}{k} \frac{1}{\sigma(1-\tau)} V, \quad (3.12a)$$

$$R_T = \frac{\mu^2}{k^2} \frac{1}{\sigma q_r (1 - \tau)} \left[\frac{q_r (m^2 - k^2) V}{\mu^2} - (2q_r + \sigma + \tau) W \right], \quad (3.12b)$$

$$R_S = \frac{\mu^2}{k^2} \frac{1}{\sigma q_r (1 - \tau)} \left[\frac{q_r (m^2 - k^2) V}{\mu^2} - (2q_r + \sigma + 1) W \right], \quad (3.12c)$$

where

$$V = 8q_r^2 + 8q_r^2(\sigma + \tau + 1) + 2q_r[(\sigma + \tau + 1)^2 + (\sigma\tau + \sigma + \tau)] + (\sigma\tau + \sigma + \tau)(\sigma + \tau + 1) - \sigma\tau,$$

$$W = -4q_r^3 + q_r[(\sigma + \tau + 1)^2 + (\sigma\tau + \sigma + \tau)] + (\sigma\tau + \sigma + \tau)(\sigma + \tau + 1) - \sigma\tau,$$

and q_r is the real part of q . By (3.5) we also obtain

$$\frac{\omega^2}{\kappa_T^2 \mu^4} = 3q_r^2 + 2q_r(\sigma + \tau + 1) + (\sigma\tau + \sigma + \tau) + \sigma \frac{k^2}{\mu^2} (R_T - R_S). \quad (3.13)$$

To find the maximum growth for the non-oscillatory mode, (3.11) must be solved simultaneously for q , k and m , for given values of ν , κ_T , κ_S , $\alpha\bar{T}_z$, $\beta\bar{S}_z$ and $\beta\bar{S}_x$. It is, however, easier to solve the equations by substituting given values of q and m/k , which then gives values for H , R_T and R_S , and hence gives the wavenumber for the maximum-growth-rate disturbance, since the Rayleigh numbers depend on the wavenumber. The equations for the oscillatory modes are solved in the same way.

The results obtained from (3.11) and (3.12) can be displayed by using a graph of $\beta\bar{S}_x/\alpha\bar{T}_z$ versus $\beta\bar{S}_z/\alpha\bar{T}_z$. For each point on the graph there is a maximum growth rate, which is given by

$$\lambda = \kappa_T \mu^2 q = \left(\frac{g\alpha|\bar{T}_z|}{\sigma} \right)^{\frac{1}{2}} \frac{q}{|R_T|^{\frac{1}{2}}}. \quad (3.14)$$

There is a maximum growth rate for both the direct and the oscillatory mode. The largest growth rate may be due to either a direct mode or an oscillatory mode. Usually we find the growth rate is largest for the direct mode, a result which also applies when $\bar{S}_x = 0$ (Baines & Gill 1969). The oscillatory mode only has a larger growth rate when \bar{T}_z is negative and $\beta\bar{S}_z/\alpha\bar{T}_z$ lies between 1 and $(\sigma + 1)/(\sigma + \tau)$, and for small values of $\beta\bar{S}_x/\alpha\bar{T}_z$. Whenever \bar{T}_z is positive, so that the temperature gradient is stable, the numerical results suggest that the non-oscillatory mode always has the largest growth rate.

For each value of $\beta\bar{S}_x/\alpha\bar{T}_z$ and $\beta\bar{S}_z/\alpha\bar{T}_z$ there corresponds a value of R_T , which gives the wavenumber for the maximum growth rate, since

$$\mu^4 = \frac{g\alpha\bar{T}_z}{\nu\kappa_T R_T}. \quad (3.15)$$

There is also a value of m/k , the slope of the wavefront to the vertical, for each value of $\beta\bar{S}_x/\alpha\bar{T}_z$ and $\beta\bar{S}_z/\alpha\bar{T}_z$.

The results obtained from (3.11) are displayed in figure 2 for the case where $\sigma = 10$ and $\tau = \frac{1}{100}$, which corresponds approximately to the diffusivities for heat and salt, and for \bar{T}_z positive. It should be noted that values of $\beta\bar{S}_z/\alpha\bar{T}_z > 1$ correspond to a gravitationally unstable basic state. We see that if $\bar{S}_z < 0$ and $\bar{T}_z > 0$ then as \bar{S}_x tends to zero m/k tends to infinity, which means the interleaving wavefronts become more horizontal, and R_T tends to infinity, so μ tends to zero.

We now look at some results we can find for any given values of σ and τ .

(i) For the direct mode, R_T has a local minimum value, which occurs when $m/k = 0$. By (3.11) this minimum value of R_T occurs when

$$q = \frac{(4(\sigma + \tau)\sigma\tau + \sigma^2\tau^2)^{\frac{1}{2}} - \sigma\tau}{2(\sigma + \tau)}. \quad (3.16)$$

The corresponding minimum value of R_T is

$$R_T = \frac{(q + 1)^2 (q(\sigma + \tau) + 2\sigma\tau)}{\sigma q(1 - \tau)}. \quad (3.17)$$

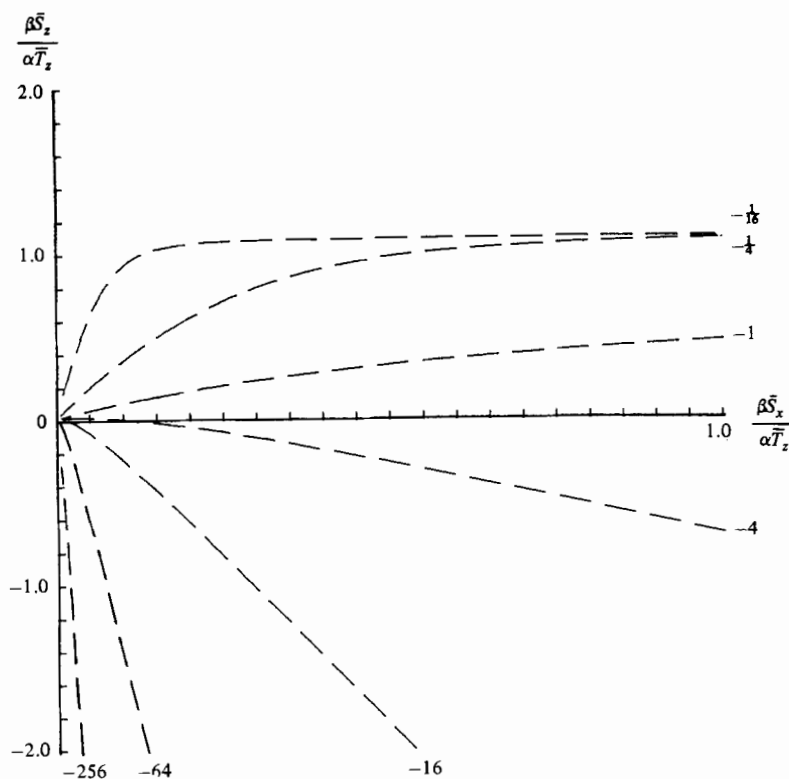
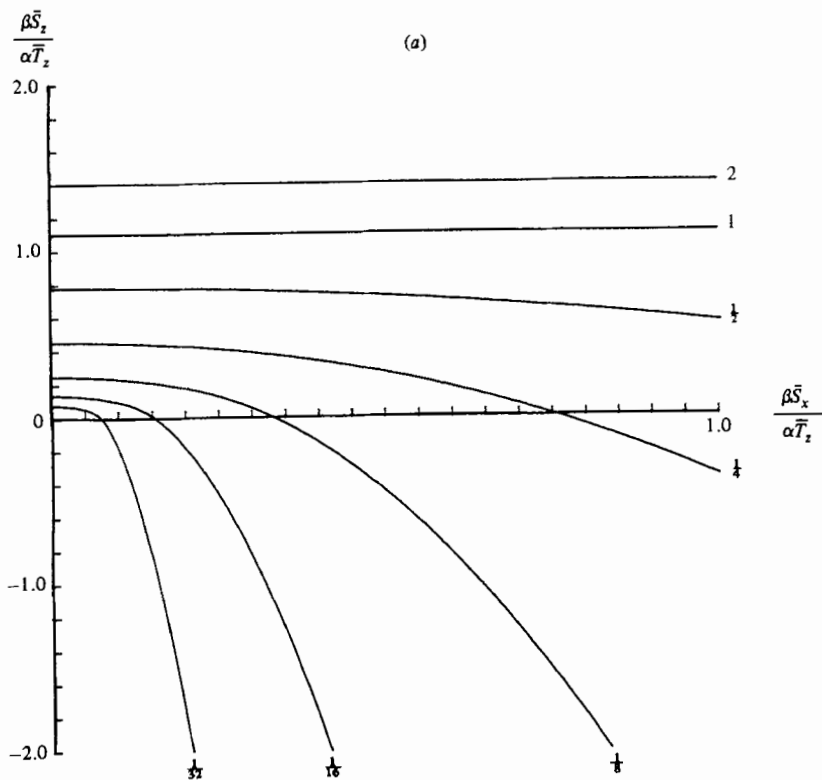


FIGURE 2(a, b). For caption see facing page.

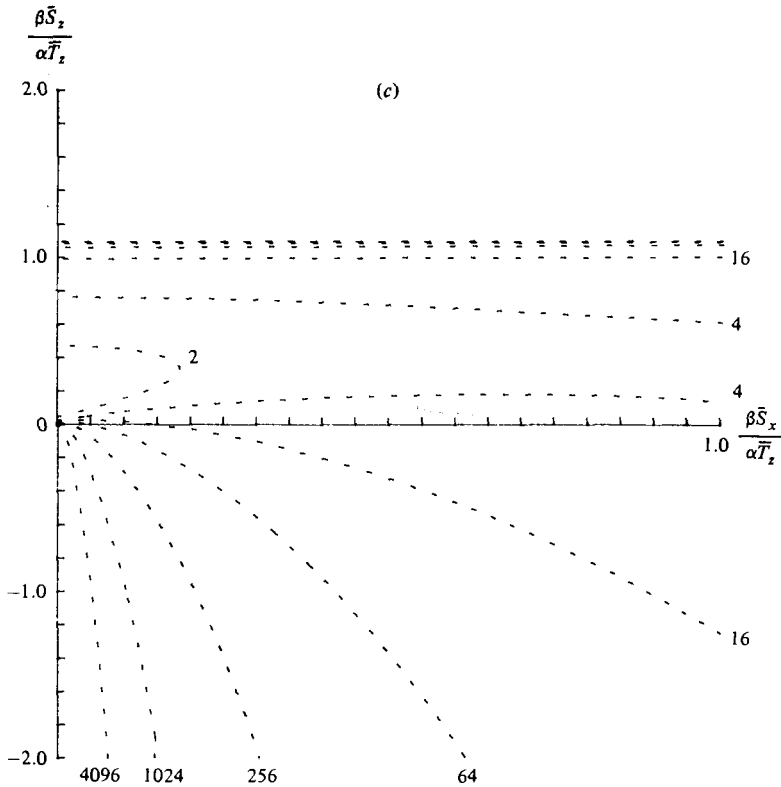


FIGURE 2. Plots of $\beta\bar{S}_z/\alpha\bar{T}_z$ versus $\beta\bar{S}_x/\alpha\bar{T}_z$ for $\bar{T}_z > 0$ when $\sigma = 10$ and $\tau = 0.01$. (a) The contours of the maximum dimensionless growth rate $q/|R_T|^{1/2}$ for the values $\frac{1}{32}, \frac{1}{16}, \frac{1}{8}, \frac{1}{4}, \frac{1}{2}, 1$ and 2 . (b) The contours of m/k corresponding to maximum growth for the values $-\frac{1}{16}, -\frac{1}{4}, -1, -4, -16, -64$ and -256 . (c) The contours of R_T corresponding to maximum growth for the values $2, 4, 16, 64, 256, 1024$ and 4096 . These contours give the wavelength, since $R_T = g\alpha\bar{T}_z/\nu\kappa_T\mu^4$.

At this point $\beta\bar{S}_x/\alpha\bar{T}_z = 0$ and

$$\frac{\beta\bar{S}_z}{\alpha\bar{T}_z} = \frac{(q + \tau)^2 (q(\sigma + 1) + 2\sigma)}{(q + 1)^2 (q(\sigma + \tau) + 2\sigma\tau)}. \tag{3.18}$$

When $\sigma = 10$ and $\tau = \frac{1}{100}$ this happens when

$$q = 0.095, \quad R_T = 1.47 \quad \text{and} \quad \beta\bar{S}_z/\alpha\bar{T}_z = 0.168.$$

The way that R_T increases away from the minimum can be seen in figure 2(c). The qualitative behaviour will be the same for all values of σ and τ , with the minimum value of R_T given by (3.17).

(ii) For positive growth rates $m/k = 0$ if and only if $\beta\bar{S}_x/\alpha\bar{T}_z = 0$ for both direct and oscillatory modes. This implies that if there is no horizontal gradient the motion with the maximum growth rate is a function of horizontal position only and that the velocity is purely vertical, as it is in salt fingering.

(iii) For the direct mode as $q \rightarrow 0$ then $\beta\bar{S}_x/\alpha\bar{T}_z \rightarrow 0$, $\beta\bar{S}_z/\alpha\bar{T}_z \rightarrow \tau$ and $R_T \rightarrow \infty$, so $\mu \rightarrow 0$. This is marginal stability for salt-fingering.

(iv) For the oscillatory mode as the real part of q tends to zero then $\beta\bar{S}_x/\alpha\bar{T}_z \rightarrow 0$, $\beta\bar{S}_z/\alpha\bar{T}_z \rightarrow (\sigma + 1)/(\sigma + \tau)$ and $R_T \rightarrow -\infty$, so $\mu \rightarrow 0$ and $\bar{T}_z < 0$. This is marginal stability for the oscillatory mode.

(v) If $q \rightarrow \infty$ and $m/k \neq 0$ then for the direct mode $\beta\bar{S}_x/\alpha\bar{T}_z \rightarrow k/m$, $\beta\bar{S}_z/\alpha\bar{T}_z \rightarrow 1$ and $R_T \rightarrow -\infty$. For the oscillatory mode $\beta\bar{S}_x/\alpha\bar{T}_z \rightarrow k/m$, $\beta\bar{S}_z/\alpha\bar{T}_z \rightarrow 1$ and $R_T \rightarrow \infty$.

(vi) If $q = A(k/m)^\alpha$ then, if α is positive, as $m/k \rightarrow 0$, $q \rightarrow \infty$. On this line, for direct modes,

$$R_T = \frac{1}{\sigma(1-\tau)} \left[-2A^3 \left(\frac{k}{m}\right)^{3\alpha-2} + A^2 \left(\frac{k}{m}\right)^{2\alpha} (\sigma + \tau) \right].$$

If $\alpha > 2$ then $R_T \rightarrow -\infty$, $\beta\bar{S}_x/\alpha\bar{T}_z \rightarrow \infty$ and $\beta\bar{S}_z/\alpha\bar{T}_z \rightarrow 1$. If $\alpha < 2$ then $R_T \rightarrow \infty$ and $\beta\bar{S}_z/\alpha\bar{T}_z \rightarrow (\sigma + 1)/(\sigma + \tau)$. If $2 > \alpha > 1$ then $\beta\bar{S}_x/\alpha\bar{T}_z \rightarrow -\infty$, and if $1 > \alpha > 0$ then $\beta\bar{S}_x/\alpha\bar{T}_z \rightarrow 0$. If $\alpha = 2$ then R_T can be positive or negative depending on whether A is smaller or larger than $\frac{1}{2}(\sigma + \tau)$. Then

$$\frac{\beta\bar{S}_z}{\alpha\bar{T}_z} = \frac{2A - (\sigma + 1)}{2A - (\sigma + \tau)},$$

$$\frac{\beta\bar{S}_x}{\alpha\bar{T}_z} = -\frac{2A^3}{\sigma(1-\tau)} \left(\frac{k}{m}\right)^5.$$

For oscillatory modes, when $q_\tau = A(k/m)^\alpha$,

$$R_T = \frac{1}{\sigma(1-\tau)} \left[8A^3 \left(\frac{k}{m}\right)^{3\alpha-2} - 4A^2 \left(\frac{k}{m}\right)^{2\alpha} (\sigma + \tau + 2) \right].$$

If $\alpha > 2$ then $R_T \rightarrow \infty$, $\beta\bar{S}_x/\alpha\bar{T}_z \rightarrow \infty$ and $\beta\bar{S}_z/\alpha\bar{T}_z \rightarrow 1$. If $\alpha < 2$ then $R_T \rightarrow -\infty$ and $\beta\bar{S}_z/\alpha\bar{T}_z \rightarrow (\sigma + 2\tau + 1)/(\sigma + \tau + 2)$. If $\alpha = 2$ then R_T is positive or negative depending on whether A is larger or smaller than $\frac{1}{2}(\sigma + \tau + 2)$. The above results are useful in obtaining and checking numerical results when $q \rightarrow \infty$ and $m/k \rightarrow 0$.

(vii) If $\alpha\bar{T}_z = 0$ then for the direct mode

$$R_S = -\left(\frac{m^2}{k^2} - 1\right) \frac{(q + \tau)(q + \sigma)}{\sigma}, \tag{3.19}$$

$$\frac{\beta\bar{S}_x}{\beta\bar{S}_z} = 2\frac{m}{k} \frac{q + 1}{\left(\frac{m^2}{k^2} - 1\right)(1 - \tau)}, \tag{3.20}$$

and $R_T = 0$, which gives an equation for m/k in terms of q :

$$(2q^3 + q^2(\sigma + \tau) - q(\sigma + \tau) - 2\sigma\tau) \frac{m^2}{k^2} = (q + 1)(q(\sigma + \tau) + 2\sigma\tau). \tag{3.21}$$

(viii) If $\beta\bar{S}_z = 0$ then for the direct mode

$$R_T = \left(\frac{m^2}{k^2} - 1\right) \frac{(q + 1)(q + \sigma)}{\sigma}, \tag{3.22}$$

$$\frac{\beta\bar{S}_x}{\alpha\bar{T}_z} = -2\frac{m}{k} \frac{q + \tau}{\left(\frac{m^2}{k^2} - 1\right)(1 - \tau)}, \tag{3.23}$$

$$(2q^3 + q(q - \tau)(\sigma + 1) - 2\sigma\tau) \frac{m^2}{k^2} = (q + \tau)(q(\sigma + 1) + 2\sigma). \tag{3.24}$$

4. Fluxes

For a propagating mode

$$\psi = \psi_0 e^{\lambda_r t} \cos(kx + mz + \lambda_1 t), \quad (4.1)$$

where we assume that ψ_0 is real. Then, by (2.5b),

$$T = \text{Re} [T_0 e^{\lambda_r t} e^{i(kx + mz + \lambda_1 t)}], \quad (4.2)$$

where

$$T_0 = \frac{im\bar{T}_x - ik\bar{T}_z}{(\lambda_r + \kappa_T \mu^2) + i\lambda_1} \psi_0, \quad (4.3)$$

$$S = \text{Re} [S_0 e^{\lambda_r t} e^{i(kx + mz + \lambda_1 t)}], \quad (4.4)$$

with

$$S_0 = \frac{im\bar{S}_x - ik\bar{S}_z}{(\lambda_r + \kappa_S \mu^2) + i\lambda_1} \psi_0. \quad (4.5)$$

The vertical convective heat flux averaged over a wavelength is given by

$$F_T = \langle wT \rangle, \quad (4.6)$$

where $\langle \rangle$ denotes an average over a wavelength, and the vertical salt flux will be

$$F_S = \langle wS \rangle. \quad (4.7)$$

Substituting from (4.1), (4.3) and (4.5) gives

$$F_T = \frac{1}{2} \frac{m\bar{T}_x - k\bar{T}_z}{(\lambda_r + \kappa_T \mu^2)^2 + \lambda_1^2} (\lambda_r + \kappa_T \mu^2) k \psi_0^2, \quad (4.8)$$

$$F_S = \frac{1}{2} \frac{m\bar{S}_x - k\bar{S}_z}{(\lambda_r + \kappa_S \mu^2)^2 + \lambda_1^2} (\lambda_r + \kappa_S \mu^2) k \psi_0^2. \quad (4.9)$$

Then, for direct modes when $\lambda_1 = 0$, we obtain the flux ratio

$$\begin{aligned} \frac{\alpha F_T}{\beta F_S} &= \frac{\alpha(k\bar{T}_z - m\bar{T}_x) (\lambda_r + \kappa_S \mu^2)}{\beta(k\bar{S}_z - m\bar{S}_x) (\lambda_r + \kappa_T \mu^2)} \\ &= \frac{(R_T - Hm/k) (q + \tau)}{(R_S - Hm/k) (q + 1)} \end{aligned} \quad (4.10)$$

By (3.11) this ratio equals

$$\frac{\alpha F_T}{\beta F_S} = \frac{(q + 1) (q(\sigma + \tau) + 2\sigma\tau)}{(q + \tau) (q(\sigma + 1) + 2\sigma)}. \quad (4.11)$$

When $\bar{S}_x = 0$ (4.10) and (4.1) give flux ratios in direct agreement with those of Schmidt (1979). The minimum value for the flux ratio is about 0.56 for $\sigma = 10$ and $\tau = 0.01$, i.e. for heat and salt, and is about 0.83 when $\sigma = 1000$ and $\tau = \frac{1}{3}$, i.e. for salt and sugar. For general σ and τ the minimum value for the flux ratio occurs when

$$q = \frac{\sigma\tau + \sigma(4\sigma^2\tau + 4\tau^2 - 2\tau(\sigma + \tau)(\sigma + 1))^{\frac{1}{2}}}{2\sigma^2 - (\sigma + \tau)(\sigma + 1)}. \quad (4.12)$$

We display the lines of constant flux ratio for the case where $\sigma = 10$ and $\tau = 0.01$ in figure 3.

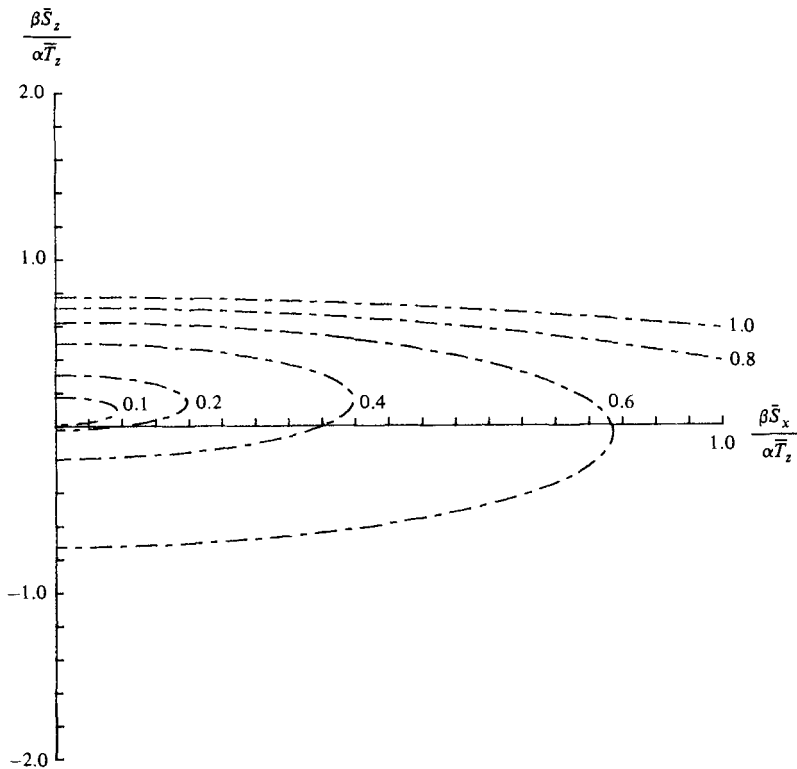


FIGURE 3. Plot of $\beta \bar{S}_z / \alpha \bar{T}_z$ versus $\beta \bar{S}_x / \alpha \bar{T}_x$ for $\bar{T}_z > 0$ when $\sigma = 10$ and $\tau = 0.01$. The lines are contours of constant flux ratio γ labelled with their values of q . When $q = 0.1$ the flux ratio γ is 0.569; when $q = 0.2$, $\gamma = 0.567$; when $q = 0.4$, $\gamma = 0.588$; when $q = 0.6$, $\gamma = 0.612$; when $q = 0.8$, $\gamma = 0.633$; and, when $q = 1.0$, $\gamma = 0.652$.

The horizontal heat flux is obtained from the vertical heat flux by

$$F_{TH} = -\frac{m}{k} F_T, \quad (4.13)$$

and the horizontal salt flux

$$F_{SH} = -\frac{m}{k} F_S. \quad (4.14)$$

The ratio of the horizontal fluxes is the same as the ratio of the vertical fluxes. It is easily shown from (4.11) that the flux ratio is always less than one. Hence salt is always transported faster than heat by this process.

The flux ratio given by (4.10) will be the appropriate value to use until salt fingers and diffusive interfaces appear. We show in § 5 why these interfaces do appear. After that stage it will be necessary to change the fluxes in order to include the presence of the salt-fingering.

5. The nonlinear solution

The full nonlinear governing equations are

$$\frac{\partial}{\partial t} \nabla^2 \psi + \mathbf{J}(\psi, \nabla^2 \psi) = \frac{\partial}{\partial x} (g(\alpha T - \beta S)) + \nu \nabla^4 \psi, \quad (5.1a)$$

$$\frac{\partial T}{\partial t} + \mathbf{J}(\psi, T) + \frac{\partial \psi}{\partial x} \bar{T}_z - \frac{\partial \psi}{\partial z} \bar{T}_x = \kappa_T \nabla^2 T, \quad (5.1b)$$

$$\frac{\partial S}{\partial t} + \mathbf{J}(\psi, S) + \frac{\partial \psi}{\partial x} \bar{S}_z - \frac{\partial \psi}{\partial z} \bar{S}_x = \kappa_S \nabla^2 S, \quad (5.1c)$$

where the Jacobian is defined by

$$\mathbf{J}(\psi, \phi) = \frac{\partial \psi}{\partial x} \frac{\partial \phi}{\partial z} - \frac{\partial \psi}{\partial z} \frac{\partial \phi}{\partial x}.$$

If the terms involving the Jacobian are removed from these equations then the linearized equations are obtained. Since all the Jacobian terms vanish identically for sinusoidal functions, any sinusoidal solution of the linearized equations will also satisfy the nonlinear equations. This is a property that also occurs for salt fingers (Huppert & Manins 1973; Holyer 1981). Therefore there is a solution to the nonlinear equations (5.1) of the form

$$\psi = \psi_0 e^{\lambda t} \cos(kx + mz), \quad (5.2a)$$

$$T = T_0 e^{\lambda t} \sin(kx + mz), \quad (5.2b)$$

$$S = S_0 e^{\lambda t} \sin(kx + mz), \quad (5.2c)$$

where ψ_0 , T_0 and S_0 are constants and we now suppose λ is real, so we have a non-oscillatory solution. Then (5.2) is a solution of (5.1) provided that

$$T_0 = \frac{k\bar{T}_z - m\bar{T}_x}{\lambda + \kappa_T \mu^2} \psi_0 \quad (5.3a)$$

and

$$S_0 = \frac{k\bar{S}_z - m\bar{S}_x}{\lambda + \kappa_S \mu^2} \psi_0, \quad (5.3b)$$

and λ satisfies the cubic equation (2.8).

We shall suppose that \bar{S}_x , ψ_0 and k are positive. There is no generality lost by making these assumptions. Then, in order that λ is positive we have, from (2.8),

$$\beta \bar{S}_x (\kappa_T - \kappa_S) \frac{m}{k} < \beta \bar{S}_z \kappa_T - \alpha \bar{T}_z \kappa_S. \quad (5.4)$$

The solution (5.2) satisfies the nonlinear equations for any values of k , m and λ that satisfy (2.8). If there is an initial disturbance in the fluid it will grow, via linear theory, with one particular wavelength growing fastest. The other modes which grow on the linear theory will be weaker than the fastest-growing mode. This solution can then carry on growing indefinitely until it, in turn, becomes unstable. This view of the growth from an initial disturbance is supported by the experiments of Ruddick & Turner (1979) and Thorpe *et al.* (1969), where periodic layers are seen, rather than many interacting modes. The growth-rate maximum is narrow enough that the variation in the thickness of the layers is small.

We now consider the case where $\bar{T}_z > 0$ and $\bar{S}_z < 0$, so both temperature and salinity are vertically stable. We also have $\kappa_T > \kappa_S$, so (5.4) implies that $m < 0$. Hence we see from (5.3) that αT_0 and βS_0 are both positive. The vertical temperature and salinity gradients given by the nonlinear solution, including the background stratifications, will be

$$T_z = \bar{T}_z + mT_0 e^{\lambda t} \cos(kx + mz), \quad (5.5a)$$

$$S_z = \bar{S}_z + mS_0 e^{\lambda t} \cos(kx + mz). \quad (5.5b)$$

Since $\bar{T}_z > 0$, $\bar{S}_z < 0$, $mT_0 < 0$ and $mS_0 < 0$, when the temperature stratification decreases, the magnitude of the salinity stratification will increase and *vice versa*. For that part of the wave with $\cos(kx + mz)$ negative (5.5) shows that the temperature stratification increases and the magnitude of the salinity stratification decreases as time passes until $S_z > 0$ and $T_z > 0$. Under these conditions one expects salt fingers to grow, starting at the level where $\cos(kx + mz) = -1$. For the part of the wave with $\cos(kx + mz)$ positive, (5.5) shows that the temperature stratification decreases and the salinity stratification increases until $T_z < 0$ and $S_z < 0$. In this region one will expect to see a diffusive interface. It is also easy to show from the velocity that warm salty intrusions sink.

Hence, in one cycle of the solution, in which $kx + mz$ changes by 2π , we expect there to be a diffusive interface and a salt-finger interface. This is seen to occur in the experiments of Ruddick & Turner (1979). The diffusive and salt-finger interfaces are not seen in the Thorpe *et al.* (1969) experiment, because the sidewalls of their tank prevent the interleaving from growing sufficiently.

The model presented in this paper will work until the salt-finger and diffusive interfaces appear. After their appearance the additional fluxes due to the salt finger will become important, as discussed by Toole & Georgi (1981). The salt fingers will have a dominant effect on the fluxes, and salt will be transported more efficiently than heat. This will change the apparent roles of the heat and the salt, because heat is now transported more slowly than salt. One can see this effect by comparing the Ruddick & Turner experiment with the Thorpe *et al.* experiment. In the Ruddick & Turner experiment, where the horizontal gradient is initially very large near the barrier, the salt-finger interfaces appear as soon as the interleaving appears, and the interleaving slopes so that warm, salty intrusions rise and cold fresh ones sink. In the Thorpe *et al.* experiment, where the horizontal gradient is close to linear across the tank, salt fingers are not observed, and the interleaving slopes so that warm salty intrusions sink and cold fresh ones rise. Hence, if the salt fingers are providing the dominant effect on the fluxes, the interleaving will slope down towards the hot salty side of the front with warm salty intrusions rising and, if the interleaving has not grown sufficiently for salt fingers to be present, the interleaving will slope up towards the hot salty side of the front with warm salty intrusions sinking.

6. Conclusions

In this paper we have presented a stability analysis for an unbounded, vertically stratified fluid which has compensating horizontal temperature and salinity gradients. We have shown that this situation is unstable and have given equations (3.11) and (3.12), which can be used to calculate the growth rate of the instability, its slope and its wavelength. Figure 2 displays these results for the case where the fluid is stratified with heat and salt, so $\sigma = 10$ and $\tau = 0.01$. We have shown the direct mode nearly always has a larger growth rate than the oscillatory mode. A solution to the full

nonlinear problem is given. It shows that the interleaving will grow until salt-finger and diffusive interfaces appear in each wavelength.

The equations (3.11) can be used to compare the theory with the experiment of Thorpe *et al.* (1969). For the experiment shown in figure 11 of their paper all the gradients are approximately linear and there is no vertical temperature, so $\alpha\bar{T}_z = 0$. Then, using (3.19)–(3.21), which are simplifications of (3.11) that apply in this special case, we find that when $\beta\bar{S}_x/\beta\bar{S}_z = -0.07$ then $q = 0.87$, $m/k = 44$ and $R_S = -1800$. This gives a wavelength, or layer depth, of approximately 2 cm, which is in good agreement with the measurement. The results obtained from (3.11), using molecular diffusivities, can strictly only be used in the early stages of interleaving, before salt-finger and diffusive interfaces appear. It is possible that, even in the ocean, interleaving could exist in this early stage. By observing the slope of the interleaving it may be possible to deduce whether or not salt fingers should be seen on the interfaces. One can obtain the order of magnitude of layer thicknesses that one expects to see in the ocean when salt fingers are present by inserting appropriate eddy diffusivities. This gives reasonable agreement with measurements of Schmitt & Georgi (1982), Fedorov (1978), Horne (1978) and Gregg (1979).

This paper describes in detail the early stages of interleaving and shows why salt-finger and diffusive interfaces appear. It is hoped it will be possible to develop the model so that the salt-finger and diffusive interfaces are included, without resorting to the crude approximation of using eddy diffusivities.

Appendix

In the analysis, we have supposed that the motion is two-dimensional. We show here that a three-dimensional perturbation is equivalent to a two-dimensional perturbation with the wavenumber of the three-dimensional motion $(k \cos \theta, k \sin \theta, m)$ replaced by $(k, 0, m)$ and the horizontal salinity gradient S_x replaced by $S_x \cos \theta$. Figure 2 shows that the maximum growth rate increases as the horizontal salinity gradient increases. Hence, when $\sigma = 10$ and $\tau = 0.01$ for any given values of \bar{T}_z , \bar{S}_z and \bar{S}_x , the two-dimensional disturbance will have the largest growth rate, because a three-dimensional disturbance is equivalent to a two-dimensional one with a smaller horizontal salinity gradient. We believe the result is true for all values of σ and τ , but have been unable to prove the result in general.

For a three-dimensional disturbance the linearized equations are

$$\nabla \cdot \mathbf{u} = 0, \tag{A 1}$$

$$\boldsymbol{\omega} = \nabla \wedge \mathbf{u}, \tag{A 2}$$

$$\frac{\partial \boldsymbol{\omega}}{\partial t} - \nu \nabla^2 \boldsymbol{\omega} = \nabla \wedge (g\hat{\mathbf{z}}(\alpha T - \beta S)), \tag{A 3}$$

$$\frac{\partial T}{\partial t} - \kappa_T \nabla^2 T = -\bar{T}_z w - \bar{T}_x u, \tag{A 4}$$

$$\frac{\partial S}{\partial t} - \kappa_S \nabla^2 S = -\bar{S}_z w - \bar{S}_x u, \tag{A 5}$$

$$\beta\bar{S}_z = \alpha\bar{T}_x, \tag{A 6}$$

where $\hat{\mathbf{z}}$ is a unit vertical vector. We look for a solution proportional to $\exp\{i\mathbf{k} \cdot \mathbf{x} + \lambda t\}$, with $\mathbf{k} = (k \cos \theta, k \sin \theta, m)$, so $\mathbf{u} = (u_0, v_0, w_0) \exp\{i\mathbf{k} \cdot \mathbf{x} + \lambda t\}$. Then the independent

equations that can be obtained from (A 1)–(A 6) are

$$k \cos \theta u_0 + k \sin \theta v_0 + m w_0 = 0, \quad (\text{A } 7)$$

$$\cos \theta v_0 = \sin \theta u_0, \quad (\text{A } 8)$$

$$(\lambda + \nu \mu^2) (k \sin \theta w_0 - m v_0) = g(\alpha T_0 - \beta S_0) k \sin \theta, \quad (\text{A } 9)$$

$$(\lambda + \kappa_T \mu^2) T_0 = -\bar{T}_z w_0 - \frac{\beta \bar{S}_x u_0}{\alpha}, \quad (\text{A } 10)$$

$$(\lambda + \kappa_S \mu^2) S_0 = -\bar{S}_z w_0 - \bar{S}_x u_0, \quad (\text{A } 11)$$

where $\mu^2 = k^2 + m^2$.

These equations then yield the characteristic equation

$$\begin{aligned} &(\lambda + \nu \mu^2) (\lambda + \kappa_T \mu^2) (\lambda + \kappa_S \mu^2) \mu^2 + \lambda g k^2 (\alpha \bar{T}_z - \beta \bar{S}_z) \\ &+ g k^2 \mu^2 \kappa_S \kappa_T \left(\frac{\alpha \bar{T}_z}{\kappa_T} - \frac{\beta \bar{S}_z}{\kappa_S} \right) + g \beta \bar{S}_x \cos \theta (\kappa_T - \kappa_S) k m \mu^2 = 0. \end{aligned} \quad (\text{A } 12)$$

This is the same as the characteristic equation (2.8) for two-dimensional perturbations, but with \bar{S}_x replaced by $\bar{S}_x \cos \theta$.

REFERENCES

- BAINES, P. G. & GILL, A. E. 1969 On thermohaline convection with linear gradients. *J. Fluid Mech.* **37**, 289.
- FEDOROV, K. N. 1978 *The Thermohaline Finestructure of the Ocean*. Pergamon.
- GREGG, M. C. 1975 Microstructure and intrusions in the California current. *J. Phys. Oceanogr.* **5**, 253.
- GREGG, M. C. 1979 Thermohaline intrusions lie across isopycnals. *Nature* **280**, 310.
- HOLYER, J. Y. 1981 On the collective stability of salt fingers. *J. Fluid Mech.* **110**, 195.
- HORNE, E. P. W. 1978 Interleaving at the subsurface front in the slope water off Nova Scotia. *J. Geophys. Res.* **83**, 3659.
- HUPPERT, H. E. & MANINS, P. C. 1973 Limiting conditions for salt fingering. *Deep-Sea Res.* **20**, 315.
- RUDDICK, B. R. & TURNER, J. S. 1979 The vertical length scale of double-diffusive intrusions. *Deep-Sea Res.* **26**, 903.
- SCHMITT, R. W. 1979 The growth rate of super-critical salt fingers. *Deep-Sea Res.* **26**, 23.
- SCHMITT, R. W. & GEORGI, D. T. 1982 Finestructure and microstructure in the North Atlantic. *J. Mar. Res.* **40**, 659.
- STERN, M. E. 1967 Lateral mixing of water masses. *Deep Sea Res.* **14**, 747.
- STOMMEL, H. & FEDOROV, K. N. 19?? Small scale structure in temperature and salinity near Timor and Mindanao. *Tellus* **19**, 306.
- THORPE, S. A., HUTT, P. K. & SOULSBY, R. 1969 The effects of horizontal gradients on thermohaline convection. *J. Fluid Mech.* **38**, 375.
- TOOLE, J. M. & GEORGI, D. T. 1981 On the dynamics and effects of double-diffusively driven intrusions. *Prog. Oceanogr.* **10**, 123.
- WALIN, G. 1964 Note on the stability of water stratified by salt and heat. *Tellus* **16**, 389.
- WIRTZ, R. A., BRIGGS, D. G. & CHEN, C. F. 1972 Physical and numerical experiments on layered convection in a density-stratified fluid. *Geophys. Fluid Dyn.* **3**, 265.